Sensors and Materials, Vol. 38, No. 2 (2026) 841–856
MYU Tokyo

S & M 4351

Multi-sensor Data-driven Collaborative Scheduling Optimization for Electric Vehicles

Zefei Chu,[1] Xuekun Hou,[1*] Ye Han,[2] and Lingling Li[3,4]

[1]College of Integrated Traditional Chinese and Western Medicine, Hebei University of Chinese Medicine, Shijiazhuang 050200, China
[2]Department of Rail Transit, Hebei Jiaotong Vocational and Technical College, Shijiazhuang 050035, China
[3]Key Laboratory of Electromagnetic Field and Electrical Apparatus Reliability of Hebei Province, Hebei University of Technology, Tianjin 300401, China
[4]State Key Laboratory of Intelligent Power Distribution Equipment and System, Hebei University of Technology, Tianjin 300401, China

(Received September 7, 2025; accepted October 21, 2025)

Keywords: electric vehicle scheduling, multimodal sensor data fusion, proximal policy optimization, microgrid operation optimization

In this study, we developed a collaborative scheduling model for electric vehicles (EVs) in smart microgrids by integrating charging pile operational monitoring data, photovoltaic (PV) output sensor data, and grid state sensing information. To address the operational optimization challenges of microgrids with high distributed energy penetration, we established an EV scheduling model. The system dynamics were characterized using a Markov decision process framework, and the proximal policy optimization algorithm was applied to optimize strategies that target maximum PV utilization. Research findings indicate that the coordinated charging of a growing EV fleet, guided by price response patterns, serves to absorb excess solar power and enhance PV utilization rates. These results validate the pivotal role of multimodal sensor data fusion in enabling the flexible regulation of power systems, while providing methodological support for optimizing sensor network deployment in the Internet of Energy Things.

1. Introduction

As the global energy structure undergoes accelerated transformation toward clean and intelligent systems, the widespread adoption of electric vehicles (EVs) and the large-scale integration of distributed renewable energy resources are profoundly reshaping traditional power system operations.(1) While EVs represent a critical flexible load resource, their charging behavior exhibits significant spatiotemporal randomness.(2) Photovoltaic (PV) generation, being weather-dependent, demonstrates inherent output volatility. The combined effect of these two factors imposes substantial challenges on smart microgrids, including intensified difficulties in supply–demand matching and the widening of load peak-valley disparities.(3) In this context, by

*Corresponding author: e-mail: houxuekun@hebcm.edu.cn
https://doi.org/10.18494/SAM5931

ISSN 0914-4935
https://myukk.org/

leveraging advanced sensing and intelligent scheduling, collaborative optimization has emerged as a pivotal solution for enhancing microgrid flexibility and renewable energy utilization.

The rapid advancement of sensor technologies provides innovative solutions to these challenges.[4] In recent years, significant performance improvements have been achieved in charging pile monitoring sensors, PV output sensing devices, and grid state perception terminals.[5] For instance, high-precision current/voltage sensors (JSMSEMI: SACS756/AHBV-4K/L3) enable the real-time monitoring of power demand fluctuations at charging stations.[6] Environmental sensors with meteorological parameter monitoring functions can provide accurate PV power generation forecasts, such as the seven-element weather sensor TH-WQX7.[7] Smart meters further enhance system awareness by delivering real-time grid load feedback.[8] The deployment of these sensing devices empowers microgrids to acquire multi-dimensional, high-resolution operational data, thereby establishing the foundation for refined scheduling and optimized energy management.[9]

Current research in the field of EV charging scheduling primarily focuses on strategies driven by a single data source. Demand response mechanisms form a core research direction, extensively utilizing price elasticity coefficient matrices to establish correlations between user behavior and price signals, guiding optimized charging behavior through dynamic pricing.[10] In terms of modeling approaches, static planning methods are employed for the simplified analysis of grid operational states and PV generation output, providing fundamental decision support for system scheduling.[11] Traditional price–response mechanisms predominantly adopt linear approximations or fixed elasticity coefficients to characterize the relationship between electricity prices and charging demand, establishing an initial coupling framework between user behavior and market signals.[12] Regarding microgrid operational characteristics, current research has examined the impact of PV's intermittent generation patterns and the spatiotemporal randomness of EV charging demands on system power balance, with studies analyzing their superposition effects.[13] In terms of technical implementation, a multi-data fusion framework integrating charging pile operational data, PV sensor information, and grid state parameters is currently being developed, with dynamic adaptive real-time scheduling strategies emerging as a key research focus to enhance microgrid operational stability under complex conditions.

Deep reinforcement learning (DRL) has emerged as a cutting-edge tool for energy system optimization due to its advantages in dynamic decision-making problems.[14] Algorithms such as Q-learning and Deep Deterministic Policy Gradient (DDPG) have been applied in scenarios including residential energy management and microgrid economic dispatch.[15] For example, Xiong *et al.*[16] demonstrated significant performance improvements in community microgrid regulation using the DDPG algorithm with an actor-critic framework for continuous action space optimization. However, traditional DRL methods suffer from overestimation bias, which leads to unstable policy convergence. To address this limitation, the twin delayed DDPG algorithm enhances training stability through dual critic networks and delayed policy updates.[17,18] The applicability of the proximal policy optimization (PPO) algorithm for coordinated EV-PV scheduling needs to be further validated in an energy system environment.

The rapid advancement of sensor technologies and materials has been instrumental in addressing these challenges. For instance, high-precision current/voltage sensors, which utilize

semiconductor-based sensing materials, enable the real-time monitoring of power fluctuations at charging stations. Similarly, environmental sensors such as the multi-parameter weather sensor, which incorporates advanced hygroscopic and thermosensitive materials, provide accurate meteorological data essential for PV generation forecasting. These sensors, coupled with smart meters equipped with micro-electromechanical systems (MEMS), form a robust sensing infrastructure that captures high-resolution, multi-dimensional operational data. In this study, we leverage such multi-source sensor data—including charging pile operational status, PV output, and grid load—to drive the collaborative scheduling of EVs, thereby enhancing the reliability and efficiency of microgrid operations.

In this study, we propose a collaborative scheduling model for EVs in smart microgrids. By integrating multi-source sensor data, the model optimizes EV charging behavior under electricity price response constraints, aiming to achieve the dual objectives of maximizing local PV consumption and minimizing grid load peak-valley differences. Research findings validate the potential of multi-source sensor data fusion in enabling flexible power system regulation, offering new insights for optimal sensor network deployment and intelligent scheduling algorithm design within the Internet of Energy Things framework. The contributions are as follows:

- In this study, we constructed a collaborative EV scheduling model for smart microgrids, integrating charging pile operational data, PV output sensor information, and grid state parameters into a multi-source data-driven framework for coordinated optimization. Building upon this foundation, a real-time scheduling strategy is proposed, which combines Markov decision process (MDP) modeling with the PPO algorithm, enabling dynamic optimization toward maximizing PV utilization.
- By developing an ordered EV charging model, we compared load peak-valley differences and PV utilization rates under various EV charging patterns and penetration levels, offering insights for system optimization.

The remaining sections are as follows. In Sect. 2, we describe the development of an EV dispatch model considering the electricity price. In Sect. 3, we develop and solve the Markov decision model. In Sect. 4, we conduct a detailed case study and analyze the simulation results. In Sect. 5, we summarize the conclusions and outlook.

2. System Model

The smart microgrid system studied in this work contains PV generation, base load, and EV charging load.

2.1 EV dispatch model considering electricity price laws

2.1.1 EV disordered charging distribution under the Monte Carlo method

The Monte Carlo method forms the analytical foundation for simulating and modeling the stochastic charging behavior of EVs. Key determinants of EV load profiles include the vehicle

owner's daily travel distance, charging initiation time, and charging termination time. Statistical analysis reveals that the probability density function governing EV daily mileage adheres to a normal distribution pattern, as mathematically expressed in Eq. (1).

$$f_d(x_d) = \frac{1}{\sqrt{2\pi} x_d \sigma_d} \exp\left[-\frac{\left(\ln x_d - \mu_d\right)^2}{2\sigma_d^2} \right] \tag{1}$$

The necessary charging power is calculated on the basis of daily travel distance, while the corresponding charging duration is subsequently determined using this power value and the charging efficiency, as mathematically represented in Eq. (2).

$$T_{charge} = \frac{f_d(x_d)}{P_{EV}^t \times \rho} \tag{2}$$

The anticipated charging initiation time exhibits a normal distribution pattern, with its corresponding probability density function mathematically represented as

$$f(t_{start}) = \frac{1}{\sqrt{2\pi}\sigma_{start}} \exp\left[-\frac{(t_{start} - \mu_{start})^2}{2\sigma_{start}^2} \right], 0 \le t_{start} \le 24. \tag{3}$$

Then, the charging end time is

$$t_{end} = t_{start} + T_{charge}. \tag{4}$$

2.1.2 EV user demand response model

Under the demand response framework, the charging behavior of EV clusters exhibits spatiotemporal shifting characteristics affected by electricity price signals. To quantify the dynamic correlation between electricity price and demand, in this section, we construct an elasticity coefficient matrix.

Assume that the scheduling period is divided into T intervals, with the electricity price vector denoted as $p^t = \left[p^{t,1}, p^{t,2} \ldots p^{t,T} \right]^\top$ and the EV charging demand vector as $p_{EV}^t = \left[p_{EV}^{t,1}, p_{EV}^{t,2} \cdots p_{EV}^{t,T} \right]^\top$. The element ε_{ij} of the elasticity coefficient matrix $E \in \mathbb{R}^{T \times T}$ represents the intensity of the effect of electricity price change at interval j on the demand at interval i.

$$\varepsilon_{ij} = \frac{\partial p_{EV}^{t,i} / p_{EV}^{t,i}}{\partial p^{t,j} / p^{t,j}} = \frac{p^{t,j}}{p_{EV}^{t,i}} \cdot \frac{\partial p_{EV}^{t,i}}{\partial p^{t,j}} \tag{5}$$

Here, ε_{ii} denotes the self-elasticity coefficient, ε_{ij} denotes the cross-elasticity coefficient, and $p_{EV}^{t,i}$ and $p^{t,j}$ represent the load and price variations at time i, respectively.

By collecting historical data from charging stations over N days, we construct a sample matrix. Within the scheduling period T, with a time interval of 1 h, the load-price elasticity coefficient matrix E^{DR} based on real-time electricity prices is formulated as

$$E^{\mathrm{DR}} = \begin{bmatrix} \varepsilon_{1,1} & \varepsilon_{1,2} & \cdots & \varepsilon_{1,T} \\ \varepsilon_{2,1} & \varepsilon_{2,2} & \cdots & \varepsilon_{2,T} \\ \vdots & \vdots & & \vdots \\ \varepsilon_{T,1} & \varepsilon_{T,2} & \cdots & \varepsilon_{T,T} \end{bmatrix}. \tag{6}$$

The change in user load after node i participates in DR is

$$\Delta P_{EV}^{t} = \begin{bmatrix} \Delta p_{EV}^{t,1} \\ \Delta p_{EV}^{t,2} \\ \vdots \\ \Delta p_{EV}^{t,T} \end{bmatrix} = \begin{bmatrix} p_{EV}^{t,1} & & & \\ & p_{EV}^{t,2} & & \\ & & \ddots & \\ & & & p_{EV}^{t,T} \end{bmatrix} E^{DR} \begin{bmatrix} \dfrac{\Delta p^{t,1}}{p^{t,1}} \\ \dfrac{\Delta p^{t,2}}{p^{t,2}} \\ \vdots \\ \dfrac{\Delta p^{t,T}}{p^{t,T}} \end{bmatrix}, \tag{7}$$

where ΔP_{EV}^{t} is the load change matrix for DR users, $\Delta p_{EV}^{t,1}$ is the load change at time $t = 1$ for node i, $p_{EV}^{t,1}$ is the initial load of node i at time $t = 1$, and $\Delta p^{t,1}$ and $p^{t,1}$ are the load change and initial electricity price, respectively, after the user participates in DR at time $t = 1$.

The relationship between the electricity price after user participation in DR and the initial electricity price, as well as the relationship between the active load after response and the initial active load, is

$$\begin{cases} p_{EV,DR}^{t,i} = p_{EV}^{t,i} - \Delta p_{EV}^{t,i}, \\ p_{DR}^{t,i} = p^{t,1}{}_{t} - p^{t,1}, \end{cases} \tag{8}$$

where $p_{EV,DR}^{t,i}$ and $p_{DR}^{t,i}$ represent the active power and electricity price after participating in demand response, respectively.

2.2 Force modeling and constraints

2.2.1 PV generation model

The PV generation model serves to simulate the operational behavior and energy output characteristics of solar PV systems. Under real-world operating conditions, the power output of

PV systems is predominantly affected by ambient temperature and solar irradiance levels. The mathematical relationship governing the output power generation can be expressed as

$$P_{PV}^{t} = A_{PV} S_G \eta_r \left[1 - \gamma_{PV} (T_s - T_{st})\right], \tag{9}$$

where the output power P_{PV}^{t} of the PV generation system is determined by the following parameters: the installed area of the PV array A_{PV}, the actual solar irradiance incident on the PV module surface S_G, the system's reference efficiency and its temperature coefficient γ_{PV}, the operating surface temperature of the PV cell T_s, and the standard temperature T_{st}.

The difference between the PV power generation and the total load of electricity consumption is reduced through EV charging scheduling, thus maximizing the PV consumption as shown in the following equations:

$$P_{pv}^{sum} = \sum_{T=0}^{23} \delta \left(P_{PV}^{t} - P_{load}^{t} - P_{EV}^{t} \right), \tag{10}$$

$$\delta = \begin{cases} 1, & P_{PV}^{t} - P_{load}^{t} - P_{EV}^{t} > 0 \\ 0, & P_{PV}^{t} - P_{load}^{t} - P_{EV}^{t} < 0 \end{cases} \tag{11}$$

where P_{EV}^{t} is the amount of EV charging at the moment T, P_{load}^{t} is the base load of the microgrid at the moment t, and δ ensures that the load will not be negative.

2.2.2 Constraints

2.2.2.1 Power balance constraint

The instantaneous generated power must equal the electrical load demand at all times.

$$P_{load}^{t} + P_{EV}^{t} + P_{PV,d}^{t} = P_{PV}^{t} + P_{pur}^{t} \tag{12}$$

Here, $P_{PV,d}^{t}$ is the abandoned solar power amount and P_{pur}^{t} is the amount of power purchased by the microgrid from the higher grid.

2.2.2.2 Electricity price constraint

Electricity tariffs must be bound within a defined range to equitably safeguard the interests of both microgrid operators and EV users.

$$p_{min}^{t} < p^{t} < p_{max}^{t} \tag{13}$$

2.2.2.3 EV charging constraints

The EV charging load during the time period t must not exceed the predefined maximum value, as mathematically constrained by Eq. (11). To guarantee that user charging requirements are fully met, the aggregate charging power of EVs participating in demand response programs must maintain equivalence with the baseline scenario without demand response participation. Furthermore, the load shifting rate is subject to operational limits defined by Eqs. (12) and (13), while the EV charging power parameter is confined within specified operational boundaries as per Eq. (14).

$$P_{EV}^{t} < P_{EV,max}^{t} \tag{14}$$

$$\sum_{t=0}^{T} P_{EV,regular}^{t} = \sum_{t=0}^{T} P_{EV,disregular}^{t} \tag{15}$$

$$\varphi_{EV} < \varphi_{EV,max} \tag{16}$$

$$SOC_{EV,min}^{n} < SOC_{EV}^{n} < SOC_{EV,max}^{n} \tag{17}$$

3. PPO-based Markov Decision Model Solving

3.1 MDP formulation

The dynamic dispatch problem of EVs absorbing PV power discussed in Sect. 3 is formulated as a MDP, a framework for modeling sequential decision-making under uncertainty. The core components of our MDP framework and their interactions are defined as follows. The Agent (the PPO-based scheduling algorithm) interacts with the Environment (the smart microgrid comprising PV, base load, and EVs). At each time step, the Agent observes the complete state of the environment (including load demand, PV output, and electricity price), based on which it selects an Action (setting the dynamic electricity price and PV curtailment level). The environment transitions to a new state, and the Agent receives a Reward that evaluates the action's effectiveness in maximizing PV consumption and minimizing grid fluctuations. This cyclic interaction of state → action → reward → next state enables the agent to learn an optimal scheduling policy through trial and error.

3.1.1 State design

In the dynamic scheduling problem of smart microgrids with EVs, the environmental state space comprises load demand P_{load}^{t}, renewable energy generation output P_{PV}^{t}, aggregate EV

charging demand P_{EV}^t, real-time electricity price p^t, and PV curtailment quantity $P_{PV,d}^t$. The state of the dynamic dispatch problem of EVs absorbing PV power is denoted as

$$s_t = \left[P_{load}^t, P_{PV}^t, P_{EV}^t, p^t, P_{PV,d}^t \right]. \tag{18}$$

3.1.2 Action design

The agent's objective is to determine optimal electricity pricing p^t and PV curtailment levels $P_{PV,d}^t$, accounting for EV charging demand being functionally dependent on electricity pricing.

$$a_t = \left[p^t, P_{PV,d}^t \right] \tag{19}$$

Here, actions $a_t \in A$ satisfy all constraints of the EV dispatch problem P1. The electricity price p^t maintains operational integrity through Eq. (10)-enforced bounds $p^t \in \left[p_{min}^t, p_{max}^t \right]$.

3.1.3 Reward function design

The agent receives a reward r_t post-action a_t. Dynamic EV scheduling leverages this instantaneous incentive to

$$r_t = \eta_1 P_{pv}^{sum} / 100 - \eta_2 \sigma_{load}^2 / 1000, \tag{20}$$

where P_{pv}^{sum} denotes total PV consumption and σ_{load}^2 represents load standard deviation. Weight coefficients η_1, η_2 balance the relative importance of these objectives, with value scaling factors /100 and /1000. The constraints inherently satisfied during action execution are excluded from the formulation. To minimize the exploration of constraint-violating decisions during agent learning, violations of Eqs. (12)–(17) trigger substantial negative penalties: a large negative constant is added to Eq. (20)'s instantaneous reward for the corresponding timestep.

3.2 PPO-based solution scheme

3.2.1 Policy interaction and trajectory generation

The PPO algorithm generates training data through real-time interactions between the agent and the environment. At each time step t, the agent samples an action a_t from the probability distribution (typically assumed as Gaussian) output by the current policy network $\pi_\theta(a \mid s)$, given the state s_t.

$$a_t \sim \pi_\theta(\cdot \mid s_t) \tag{21}$$

Unlike off-policy algorithms, PPO adopts an on-policy learning mechanism, requiring the historical interaction data to be cleared after each policy update and replaced with newly collected trajectories $\tau = \{s_t, a_t, r_t, s_{t+1}\}$. While this imposes higher demands on real-time exploration, it avoids distributional shifts induced by experience replay mechanisms.

3.2.2 Advantage estimation and objective function design

The core of PPO lies in its clipped surrogate objective, which stabilizes policy updates by constraining the divergence between old and new policies. First, the state value is estimated using the critic network $V_\phi(s)$, and the generalized advantage estimation computes the advantage values.

$$\hat{A}_t = \sum_{l=0}^{T-t} (\gamma\lambda)^l \delta_{t+l}, \quad \delta_t = r_t + \gamma V_\phi(s_{t+1}) - V_\phi(s_t) \tag{22}$$

Here, $\lambda \in [0,1]$ balances bias and variance, and γ is the discount factor.

The policy update objective restricts the ratio of new-to-old policy probabilities to prevent abrupt policy changes.

$$\mathcal{L}^{CLIP}(\theta) = \mathbb{E}_t\left[\min\left(\frac{\pi_\theta(a_t \mid s_t)}{\pi_{\theta_{old}}(a_t \mid s_t)}\hat{A}_t, clip\left(\frac{\pi_\theta(a_t \mid s_t)}{\pi_{\theta_{old}}(a_t \mid s_t)}, 1-\epsilon, 1+\epsilon\right)\hat{A}_t\right)\right] \tag{23}$$

Here, ϵ is the clipping threshold that truncates extreme probability ratios to ensure smooth policy updates. The critic network is optimized by minimizing the mean squared error of the value function.

$$\mathcal{L}^{VF}(\phi) = \mathbb{E}_t\left[\left(V_\phi(s_t) - \hat{R}_t\right)^2\right], \quad \hat{R}_t = \sum_{l=0}^{T-t} \gamma^l r_{t+l} \tag{24}$$

To enhance exploration, an entropy regularization term $H(\pi_\theta(\cdot \mid s_t))$ can be incorporated, forming a composite loss function.

$$\mathcal{L} = \mathcal{L}^{CLIP} + c_1\mathcal{L}^{VF} - c_2\mathbb{E}_t\left[H(\pi_\theta(\cdot \mid s_t))\right] \tag{25}$$

3.2.3 Mini-batch multi-epoch parameter updates

PPO employs the mini-batch multi-epoch gradient ascent to improve data efficiency. Specifically, complete trajectories are divided into mini-batches, and gradients are computed iteratively over 3–4 epochs to fully exploit the data. This mechanism mitigates the low data efficiency inherent in on-policy algorithms while preventing overfitting through limited update cycles.

4. Case Analysis

4.1 Basic data

In this study, we employed real-world operational data from a Hebei Province, China microgrid (2023) with 24 h dispatch cycles ($T = 24$) at 1 h resolution. PV generation, base load, electricity pricing, and EV charging datasets represent actual recorded values. To assess PPO algorithm robustness within this framework, a solar curtailment penalty of 0.6 CNY/kWh is implemented. To quantify the interdependencies between different EVs, the correlation coefficients are presented in Table 1. The EV maximum load transfer rate is set to 0.3, considering the factor of EV charging satisfaction. The electricity price for uncoordinated charging is 0.8 CNY/(kWh).

4.2 Training process

All experiments were executed with a fixed random seed (42) applied to Python, NumPy, and PyTorch; the dataset comprises real operational records from a Hebei Province microgrid in 2023 covering 24 h dispatch cycles ($T = 24$) at 1 h resolution, including PV generation, base load, electricity price, and EV charging. The data processing pipeline is as follows: PV power is obtained from hourly irradiance/temperature measurements and converted via the PV model; load series are normalized (per-unit) with short gaps linearly interpolated to maintain hourly alignment; electricity price follows recorded time-of-use tariffs with any missing values linearly interpolated; and EV charging demand is generated via a Monte Carlo procedure consistent with observed travel distance, arrival time, and charging duration distributions. These steps enable the faithful replication and extension of our results under identical settings.

The simulations in this study are executed in Python 3.9.19 on a computer with an Intel Core i5-12400F @2.50 GHz CPU and 16 GB of RAM. The proposed PPO algorithm employs two deep neural networks: an actor network for stochastic policy parameterization and a critic network for state-value estimation. Both networks share identical hidden layer architectures, consisting of an input layer, two fully connected hidden layers with 200 neurons each, and rectified linear unit activation functions. The actor network processes the state space vector and outputs parameters of a Gaussian distribution—specifically, the mean and log standard deviation

Table 1
EV parameters.

Parameter	Value	Unit
Average charge/discharge power	5	KW
Charge and discharge efficiency	0.9	%
Maximum daily mileage	350	kM
Battery capacity	45	kWh
Power consumption	7.5	km/kWh
SOC_{up}^{EV}	100	%
SOC_{down}^{EV}	20	%

for each action dimension. The mean values are linearly activated to span the continuous action space, while the log standard deviation is optimized independently to control exploration. Key hyperparameters include a discount factor $\gamma = 0.99$, a generalized advantage estimation coefficient $\lambda = 0.95$, and a clipping threshold $\epsilon = 0.2$ to constrain policy updates. The actor and critic networks utilize Adam optimizers with learning rates of 3×10^{-4} and 1×10^{-3}. Entropy regularization with a coefficient of 0.01 is applied to encourage exploration, penalizing overly deterministic policies. Training proceeds via mini-batch gradient ascent over four epochs per iteration, with a batch size of 64 trajectories. Observation normalization is implemented using running mean and standard deviation to mitigate input scaling sensitivity, while early stopping halts training if the average reward plateaus within a 1% tolerance for 10 consecutive epochs.

Figure 1 shows the convergence of the PPO scheduling algorithm through the training reward curve. During initial exploration, the agent yields low immediate rewards due to the limited prior knowledge of the environment. As training progresses, accumulated state-action experience drives gradual performance improvement. The reward curve stabilizes after 1000 episodes, maintaining an average value of −1300, which confirms policy optimization convergence and indicates the successful derivation of a near-optimal EV scheduling strategy.

4.3 Case setting

In this study, we established two scenarios with 400 and 600 EVs to analyze the impact of EV quantity on PV consumption. By comparing two strategies within each scenario, we investigate how different charging strategies affect PV utilization. The analysis employs PV generation profiles and baseline load data from a typical summer day.

Strategy 1: Coordinated EV charging based on time-of-use electricity pricing

Strategy 2: Uncoordinated EV charging

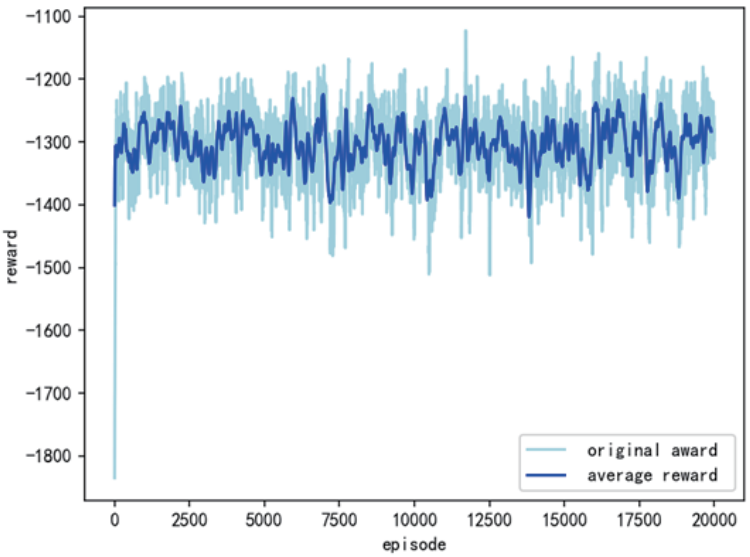

Fig. 1. (Color online) Reward curve for the training process.

In this section, we present simulation results of both uncoordinated and coordinated EV charging loads. A comparative analysis is conducted to evaluate variations in PV consumption levels and load peak-valley differences across distinct charging scenarios.

In this study, the peak load is defined as the maximum hourly load within the 24 h dispatch cycle, and the valley load is the minimum hourly load value within the same cycle. No additional smoothing was applied. The PV consumption was calculated as the total PV energy absorbed by EV charging and base load, integrated over the entire 24 h scheduling horizon.

Figure 2 shows the load curves and charging volumes under coordinated and uncoordinated charging cases for both EV fleet sizes. In Fig. 2(a), uncoordinated charging exhibits concentrated power demand during 18:00–20:00 when the PV output is minimal, resulting in underutilized solar generation. The coordinated strategy effectively shifts charging activities to midday peak PV production hours, enhancing solar consumption efficiency. Figure 2(b) shows that with increased EV adoption, the disparity between coordinated and uncoordinated load profiles widens further, as higher charging volumes amplify the PV consumption improvement achieved through strategic scheduling.

Quantitative evaluations of key performance indicators are presented in Table 2, using annual charging cost data and summer seasonal load profiles. Uncoordinated charging exacerbates peak-hour congestion by aligning with existing residential demand patterns, creating dual-peak stress on grid operations. The late-evening peak tariff period (highest electricity price)

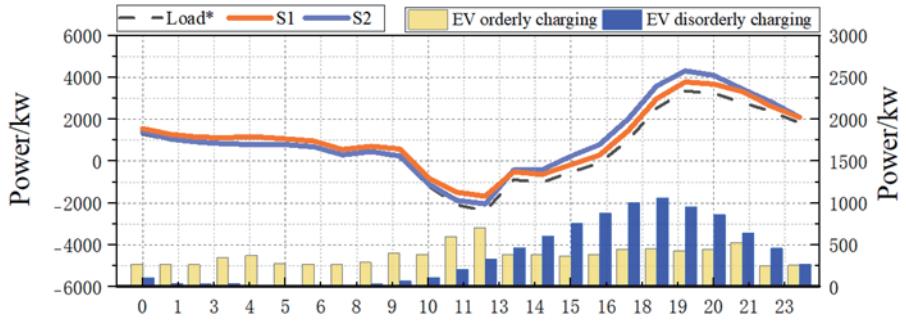

(a)

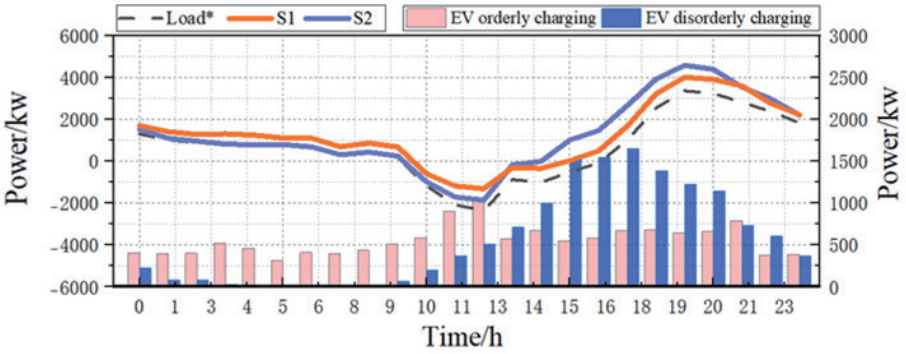

(b)

Fig. 2. (Color online) Comparison of different strategic load profiles and EV charging in two scenarios. (a) 400 EVs. (b) 600 EVs.

Table 2
Comparison of parameters in different scenarios.

Parameter	Strategy 1 (case 1)	Strategy 2 (case 1)	Strategy 1 (case 2)	Strategy 2 (case 2)
Annual costs for EV users (CNY)	6088865	6488540	10058325	10805825
PV consumption (kWh)	18119	15605	21912	18324
PV in situ consumption rate (%)	54.84	47.23	66.32	55.46
Peak load (kW)	3944	4554	4170	4880
Load valley (kW)	1091	801	1128	780

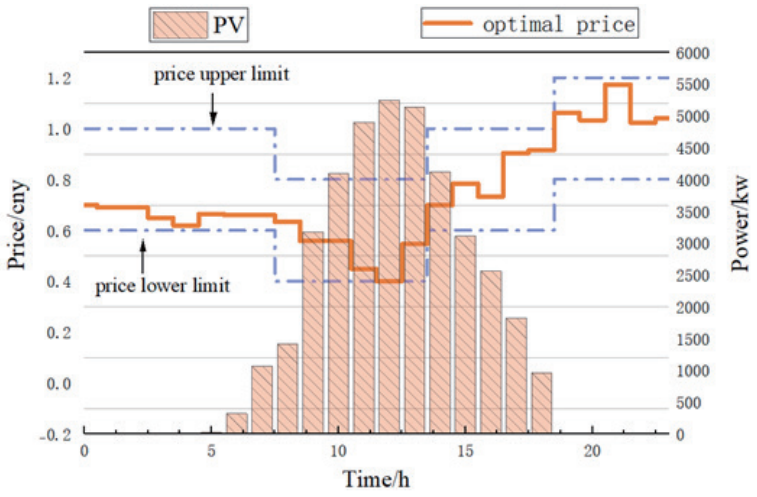

Fig. 3. (Color online) Dynamic tariffs under strategy 1.

contributes to elevated charging costs, with total uncoordinated charging expenses reaching 6488540 CNY in case 1. Figure 3 shows the 24 h dynamic pricing under Strategy 1, showing significant charging load migration to 11:00–13:00 when both solar generation and pricing are optimal. This dual optimization achieves 2514 kW incremental PV consumption and 610 kWh peak load reduction compared with Strategy 2, while decreasing the peak-valley difference by 900 kW. The coordinated approach demonstrates dual benefits: 399675 CNY cost savings through valley-hour charging utilization and enhanced grid stability via peak-shaving and valley-filling effects. These results confirm that strategic EV charging management simultaneously improves renewable integration and operational efficiency in power systems.

Building upon case 1, case 2 further increases the number of EVs. With the growth of charging load, the prescheduling PV consumption rate in case 2 rises to 55.46%, higher than 47.23% in case 1. However, uncoordinated charging leads to further elevation of grid load peaks. After superimposing disorganized EV charging, the total load peak in case 2 reaches 4880 kW. Through the scheduling and management of EV charging loads, the total peak load decreases to 4170 kW, while the PV consumption rate improves to 66.32%, representing a 10.86% increase compared with the unscheduled condition. With the expansion of total schedulable loads, the potential for PV consumption shows significant enhancement. Therefore, the increased EV penetration rate in this region contributes to improved PV consumption levels.

In summary, uncoordinated EV charging creates peak-on-peak phenomena in the power grid, imposing higher requirements for supply stability and reliability. As an excellent adjustable load resource, EVs demonstrate multiple functions when fully utilizing their load characteristics. The reasonable scheduling of EV charging times can simultaneously enhance PV utilization and reduce grid peak-valley differences. The comparative analysis of scheduling results under different EV charging mode ratios and penetration rates indicates that coordinated charging based on electricity price response mechanisms, when combined with increased EV adoption, will further enhance the PV consumption ratio.

5. Conclusions

In this study, we proposed a multi-source sensor data-driven coordinated scheduling framework for EVs in smart microgrids to address operational challenges posed by high-penetration distributed energy resources. On the basis of charging station operational data, EV mobility patterns under the effects of electricity price were derived. By integrating PV output sensor data and grid status parameters, the MDP-based EV scheduling model was designed to optimize system dynamics under various renewable energy conditions. Using the PPO algorithm, the proposed framework maximizes local PV consumption while maintaining grid stability. Comparative analyses were conducted on PV consumption ratios and load peak-valley differences across different EV charging modes and penetration rates. The key conclusions are summarized as follows:

(1) The PPO-based MDP framework demonstrates exceptional adaptability in dynamic environments, exhibiting rapid convergence characteristics during training: The algorithm's reward values stabilized after approximately 1000 training episodes in test scenarios, highlighting DRL's potential for complex energy management tasks.
(2) Uncoordinated EV charging exacerbates grid load peak-valley differences by 23.98%, while coordinated charging management not only mitigates this disparity but also enhances PV consumption by 2514 kWh. The potential for PV consumption further increases with higher EV penetration rates.

In conclusion, in this research, we established theoretical foundations and practical pathways for smart microgrid flexibility through the deep integration of multi-source sensor data and EV scheduling models. Future investigations will focus on developing more effective EV incentive mechanisms and optimizing energy storage configurations to achieve higher renewable energy utilization rates.

Acknowledgments

This study was supported by the Tianjin Carbon Peak and Carbon Neutrality Technology Major Project (Grant No. 24ZXTKSN00030).

References

1 Z. W. Zhong, W. Y. Hu, and X. L. Zhao: Appl. Energy **361** (2024) 122904. https://doi.org/10.1016/j.apenergy.2024.122904
2 Z. C. Yang, F. Yang, H. D. Min, H. Tian, W. Hu, J. Liu, and N. Eghbalian: Energy **263** (2023) 125695. https://doi.org/10.1016/j.energy.2022.125695
3 S. H. Zhao, K. Li, Z. L. Yang, X. Z. Xu, and N. Zhang: Appl. Energy **314** (2022) 118715. https://doi.org/10.1016/j.apenergy.2022.118715
4 N. Kumar: IEEE Trans. Energy Convers. **39** (2024) 29. https://doi.org/10.1109/tec.2023.3298817
5 D. Zhang, D. Wang, Z. Xu, X. Zhang, Y. Yang, J. Guo, B. Zhang, and W. Zhao: Coord. Chem. Rev. **427** (2021) 213597. https://doi.org/10.1016/j.ccr.2020.213597
6 Z. Duan, M. Zhang, Y. Jiang, Z. Yuan, and H. Tai: J. Mater. Chem. A **12** (2024) 14975. https://doi.org/10.1039/d3ta06283j
7 N. Kumar, B. Singh, and B. K. Panigrahi: IEEE Trans. Transp. Electrif. **9** (2023) 2583. https://doi.org/10.1109/tte.2022.3213253
8 K. Wang, X. Lin, F. Wei, and H. Wei: IEEE Access. **12** (2024) 1483. https://doi.org/10.1109/access.2023.3347425
9 B. Liu, J. Zhang, W. Luan, B. Zhao, Z. Liu, and Y. Yu: IEEE Trans. Instrum. Meas. **73** (2024) 2502514. https://doi.org/10.1109/tim.2023.3341128
10 C. Y. Yang, Y. Zhao, X. T. Li, and X. Zhou: Renewable Energy **238** (2025) 121890. https://doi.org/10.1016/j.renene.2024.121890
11 H. Kuang, X. Zhang, H. Qu, L. You, R. Zhu, and J. Li: Sustainable Cities Soc. **115** (2024) 105836. https://doi.org/10.1016/j.scs.2024.105836
12 A. P. Kaur and M. Singh: Energy **273** (2023) 127243. https://doi.org/10.1016/j.energy.2023.127243
13 G. P. Wu, C. Yi, H. Xiao, Q. W. Wu, L. J. Zeng, Q. Yan, and M. L. Zhang: IEEE Trans. Smart Grid **14** (2023) 4322. https://doi.org/10.1109/TSG.2023.3250722
14 S. I. Abouzeid, Y. Chen, M. Zaery, M. A. Abido, A. Raza, and E. H. Abdelhameed: Comput. Electr. Eng. **123** (2025) 110093. https://doi.org/10.1016/j.compeleceng.2025.110093
15 Y. Y. Wan, H. C. Zhang, Y. Y. Hu, Y. B. Wang, X. S. Liu, Q. Zhou, and Z. Chen: Energy **313** (2024) 133907. https://doi.org/10.1016/j.energy.2024.133907
16 K. Xiong, Q. L. Wei, and Y. Liu: IEEE Trans. Smart Grid **16** (2025) 1051. https://doi.org/10.1109/TSG.2024.3461320
17 C. Wang, J. Zhang, A. Wang, Z. Wang, N. Yang, Z. Zhao, C. S. Lai, and L. L. Lai: Appl. Energy **368** (2024) 123471. https://doi.org/10.1016/j.apenergy.2024.123471
18 D. Dominguez-Barbero, J. Garcia-Gonzalez, M. A. Sanz-Bobi, and A. Garcia-Cerrada: Appl. Energy **368** (2024) 123435. https://doi.org/10.1016/j.apenergy.2024.123435

About the Authors

Zefei Chu holds a master's degree and currently serves as a lecturer at Hebei University of Chinese Medicine. Her research interests include the reliability analysis of power systems and digital image processing.
(chuzefei@hebcm.edu.cn)

Xuekun Hou holds a master's degree and currently serves as a lecturer at Hebei University of Chinese Medicine. His research interests include the control and reliability analysis of electromechanical systems.
(houxuekun@hebcm.edu.cn)

Ye Han holds a master's degree and currently serves as a lecturer at Hebei Jiaotong Vocational and Technical College. Her research interests include the reliability analysis of power systems and optimization technology for reactive power compensation in substations. (han201709002@hejtxy.edu.cn)

Lingling Li received her M.S. degree in control theory and control engineering in 2001 and her Ph.D. degree in electrical machinery and appliances in 2004 from Hebei University of Technology. She is currently a professor at the School of Electrical Engineering, Hebei University of Technology, and a permanent member of the State Key Laboratory of Reliability and Intelligence of Electrical Equipment. Her research interests include power systems, new energy, and electrical reliability.
(lilingling@hebut.edu.cn)